Supplementary information:

Mechanistic insights into peptide and ligand binding of ATAD2-bromodomain via atomistic simulations disclose a role of induced fit and conformational selection

Yang Zhou [a†], Muzammal Hussain [b, c†], Guanglin Kuang [a], Jiancun Zhang [b, c *], and Yaoquan Tu [a *]

[a] Division of Theoretical Chemistry and Biology, School of Biotechnology, Royal Institute of Technology (KTH), AlbaNova University Center, Stockholm, 10691, Sweden

[b] Guangdong Provincial Key Laboratory of Biocomputing, Institute of Chemical Biology, Guangzhou Institutes of Biomedicine and Health, Chinese Academy of Sciences, Guangzhou 510530, China

[c] University of Chinese Academy of Sciences, No. 19 Yuquan Road, Beijing, 100049, PR China

*** Corresponding authors**:

Yaoquan Tu, Division of Theoretical Chemistry and Biology, School of Biotechnology, Royal Institute of Technology (KTH), AlbaNova University Center, Stockholm, 10691, Sweden

Tel.: +46 8 790 96 45
Email: Y. Tu (yaoquan@kth.se)

Jiancun Zhang, Guangzhou Institutes of Biomedicine and Health, Chinese Academy of Sciences, 190 Kaiyuan Avenue, Science Park, Guangzhou, 510530, PR China

Tel.: +86 020 32015323
Email: J. Zhang (zhang_jiancun@gibh.ac.cn)

[†] These authors contributed equally to this work

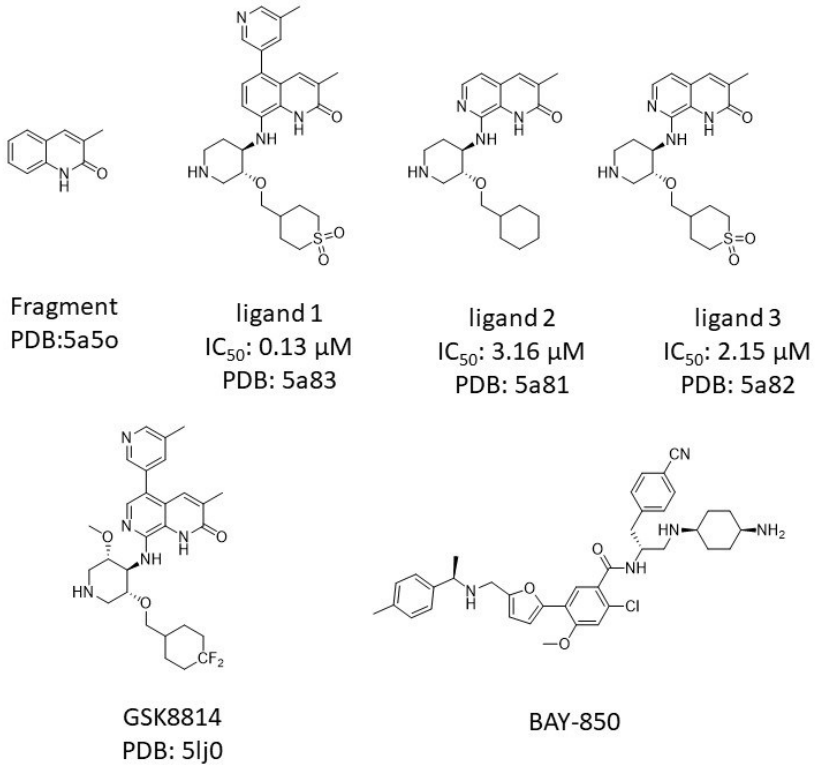

Figure S1. Chemical structures of ATAD2's BRD ligands. IC_{50} values are taken from experimental affinity measurement [1-4]

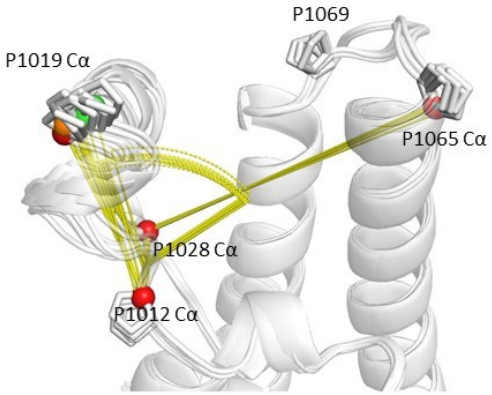

Figure S2. Superposition of selected PDB structures to highlight differences in ZA loop positioning, and illustration of the ZA dihedral measurement criteria among the Cα-atoms of specific proline residues (PDBs: 3dai, 4qsp, 4qsx, 4qut, 4tt2, 4tu6, 5a5n, 5a5r, 5a81, 5a82, 5a83)

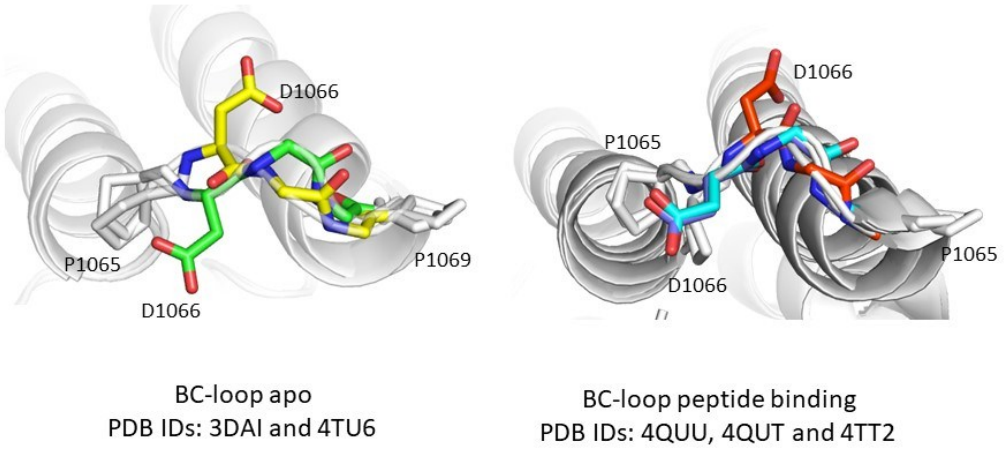

Figure S3. Superposition of selected PDB structures to show alternate conformations ("in" and "out") of the BC loop, which can be distinguished by the side-chain conformations of Asp1066 (D1066) pointing, respectively, within and outside the binding pocket. Left: apo form structures (PDBs: 3dai and 4tu6), right: peptide-bound structures (PDBs: 4quu, 4qut and 4tt2).

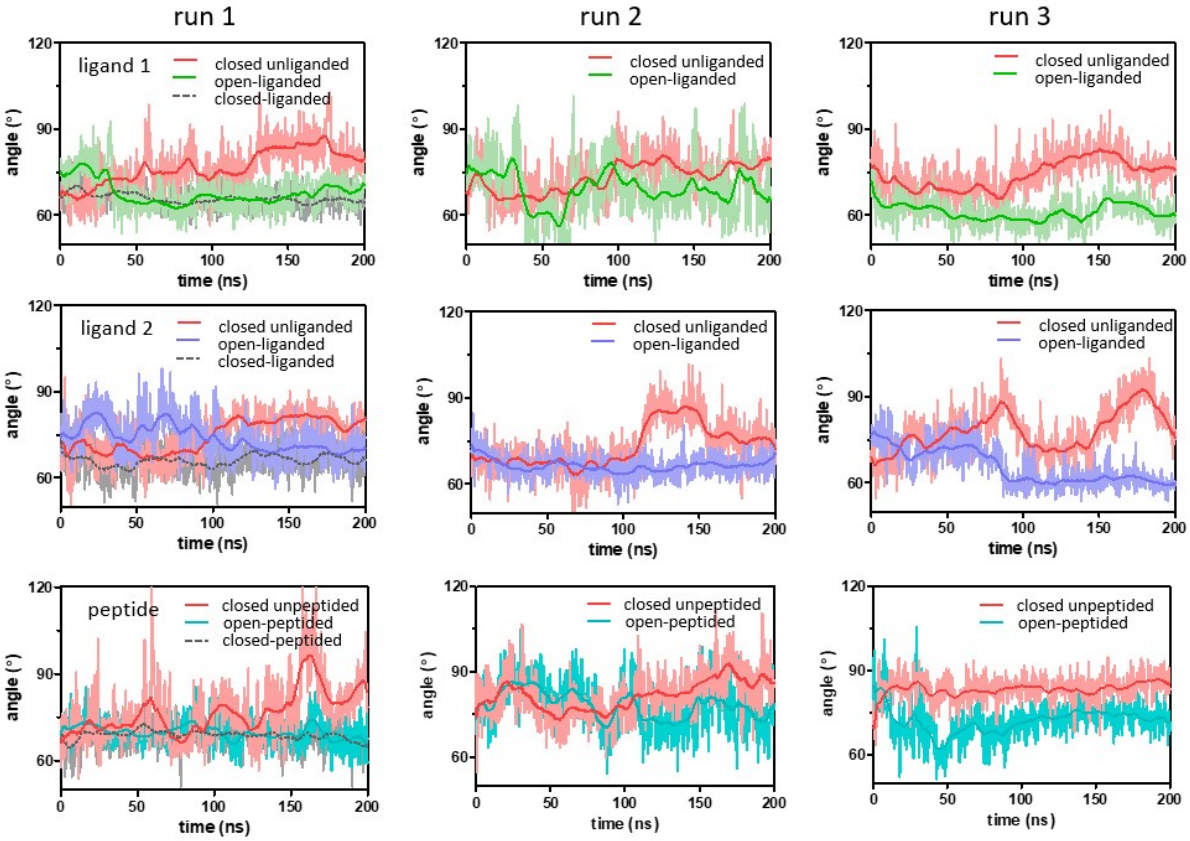

Figure S4. Dihedral angle evolution in three independent MD simulations.

Figure S5. Sitemap prediction of the helix binding region. Yellow surface: hydrophobic region, red surface: acceptor region, blue surface: donor region. Yellow dash line represents thehydrogen bond and the green dash line pi-pi stacking interaction.

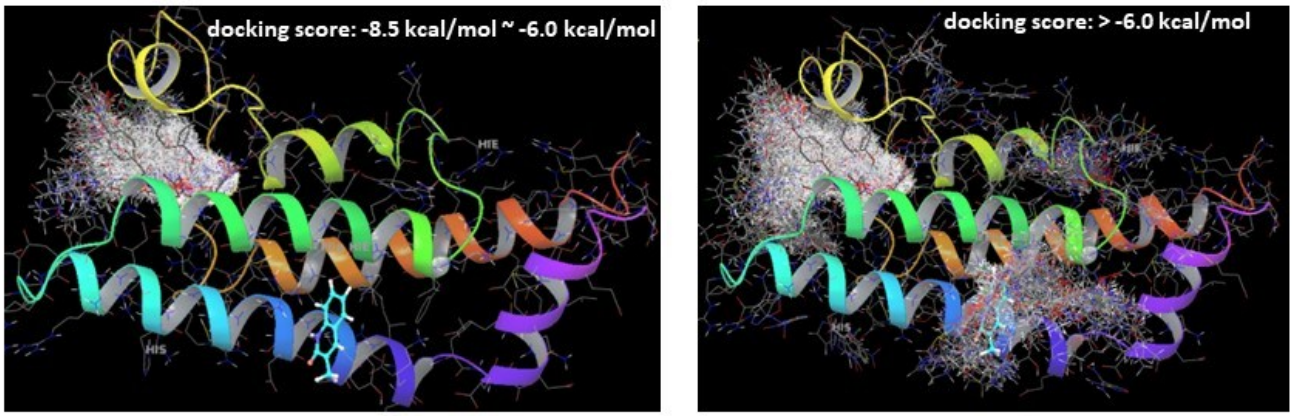

Figure S6. Blind docking results of the SPECS building blocks library.

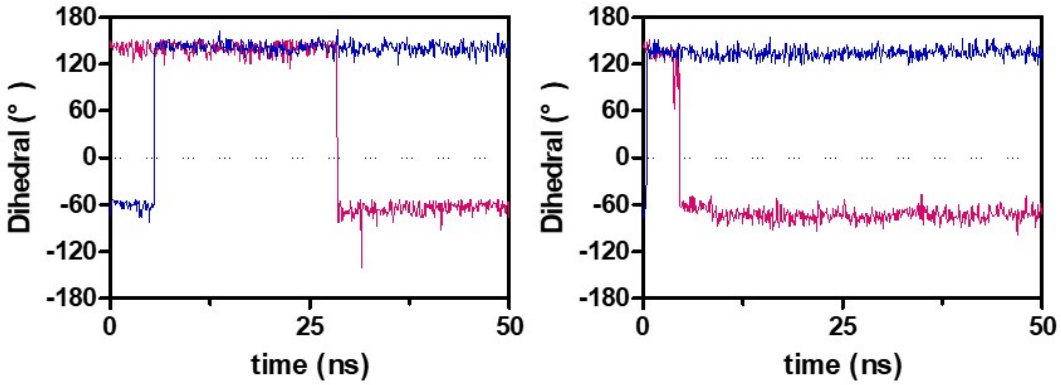

Figure S7 Evolution of the dihedral χ_2 in two additional independent simulations.

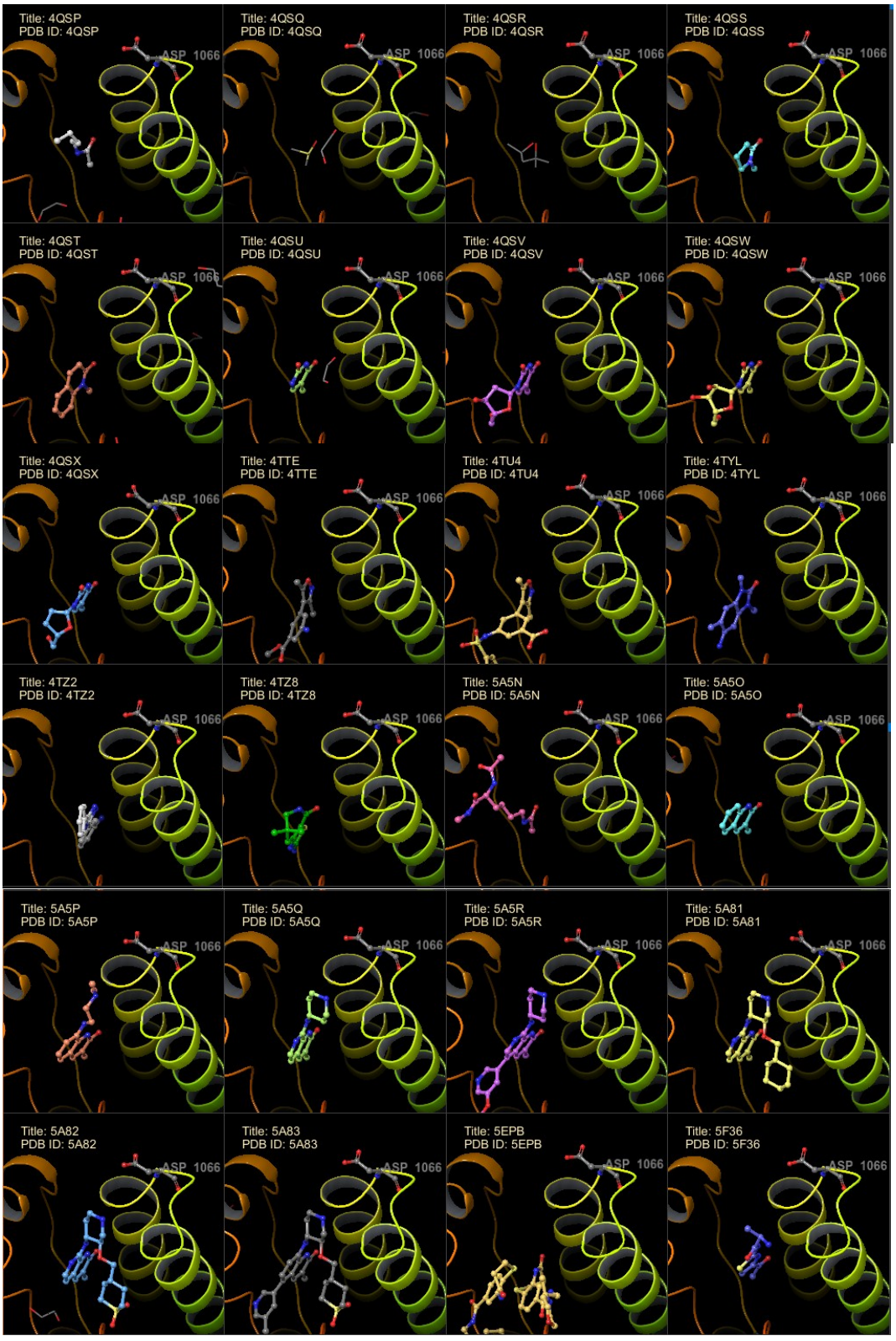
Title: 4QSP
PDB ID: 4QSP
Title: 4QSQ
PDB ID: 4QSQ
Title: 4QSR
PDB ID: 4QSR
Title: 4QSS
PDB ID: 4QSS
Title: 4QST
PDB ID: 4QST
Title: 4QSU
PDB ID: 4QSU
Title: 4QSV
PDB ID: 4QSV
Title: 4QSW
PDB ID: 4QSW
Title: 4QSX
PDB ID: 4QSX
Title: 4TTE
PDB ID: 4TTE
Title: 4TU4
PDB ID: 4TU4
Title: 4TYL
PDB ID: 4TYL
Title: 4TZ2
PDB ID: 4TZ2
Title: 4TZ8
PDB ID: 4TZ8
Title: 5A5N
PDB ID: 5A5N
Title: 5A5O
PDB ID: 5A5O
Title: 5A5P
PDB ID: 5A5P
Title: 5A5Q
PDB ID: 5A5Q
Title: 5A5R
PDB ID: 5A5R
Title: 5A81
PDB ID: 5A81
Title: 5A82
PDB ID: 5A82
Title: 5A83
PDB ID: 5A83
Title: 5EPB
PDB ID: 5EPB
Title: 5F36
PDB ID: 5F36
ASP 1066

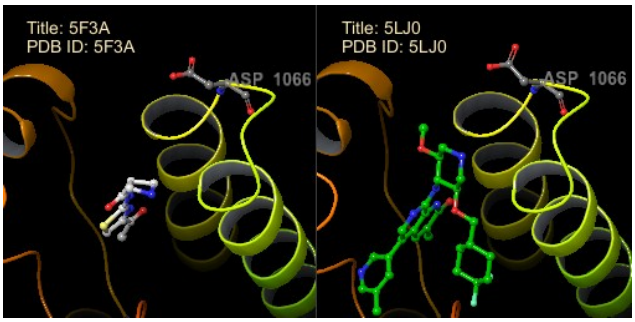

Figure S8. Residue Asp1066 in all the currently available fragment- and inhibitor- bound complexes of ATAD2's BRD. (PDBs: 4qsp, 4qsq, 4qsr, 4qss, 4qst, 4qsu, 4qsv, 4qsw, 4qsx, 4tte, 4tu4, 4tyl, 4tz2, 4tz8, 5a5n, 5a5o, 5a5p, 5a5q, 5a5r, 5a81, 5a82, 5a83, 5epb, 5f36, 5f3a, 5lj0)

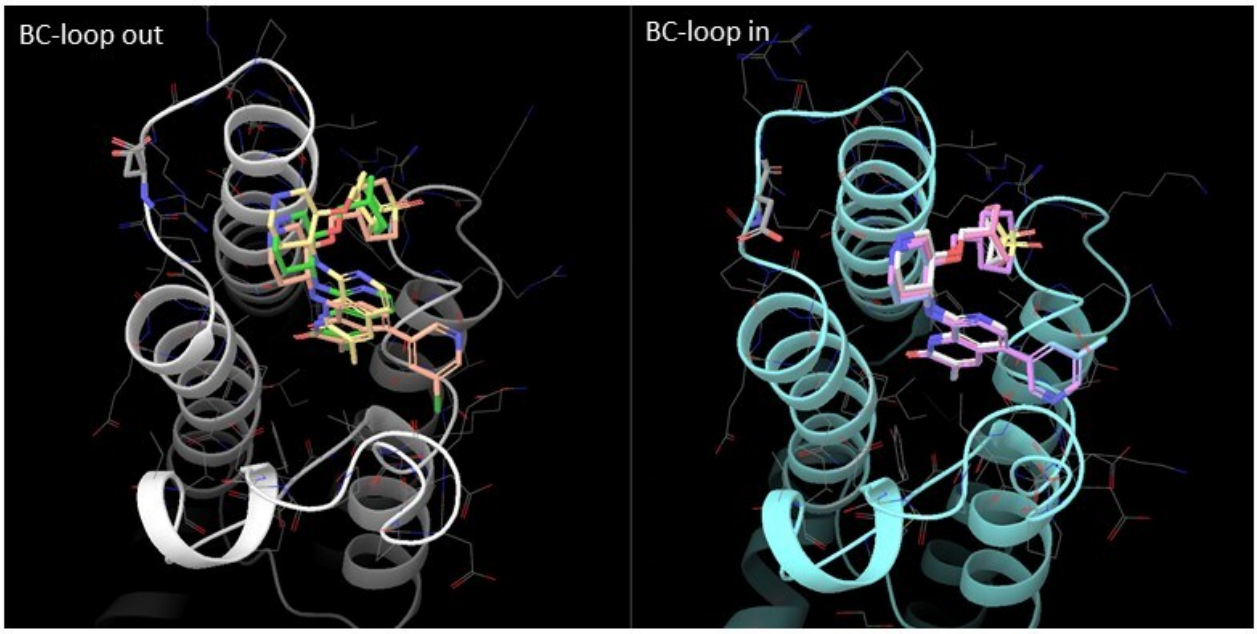

Figure S9. Docking poses of ligands in the BC loop "in" and "out" conformations.

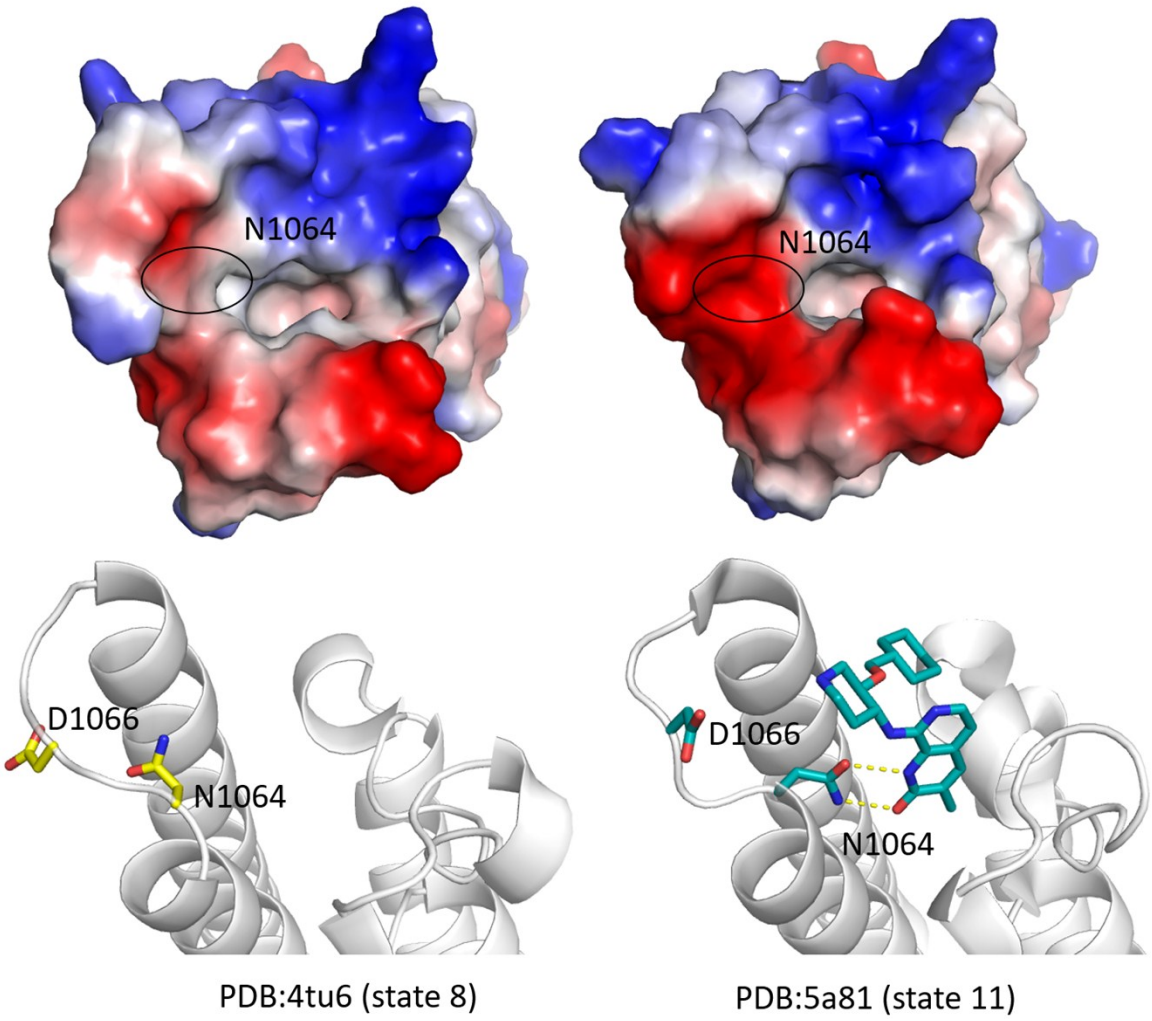

Figure S10. Impact of Asn1064 (N1064) flipping event on the binding pocket geometry

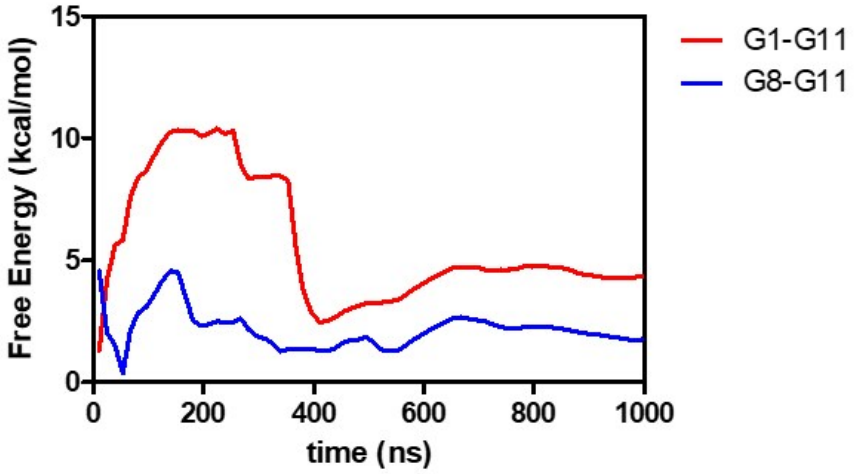

Figure S11. Free energy difference as a function of simulation time. Red: free energy difference between state 1 and state 11 (G_1-G_{11}); Blue: free energy difference between sate 8 and state 11 ($G_8 - G_{11}$).

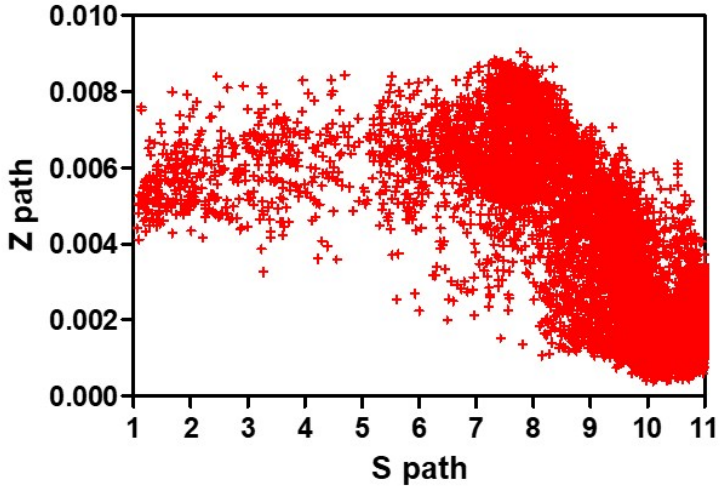

Figure S12. The distance from the path (Z_{path}) vs. the progress along the path (S_{path}).

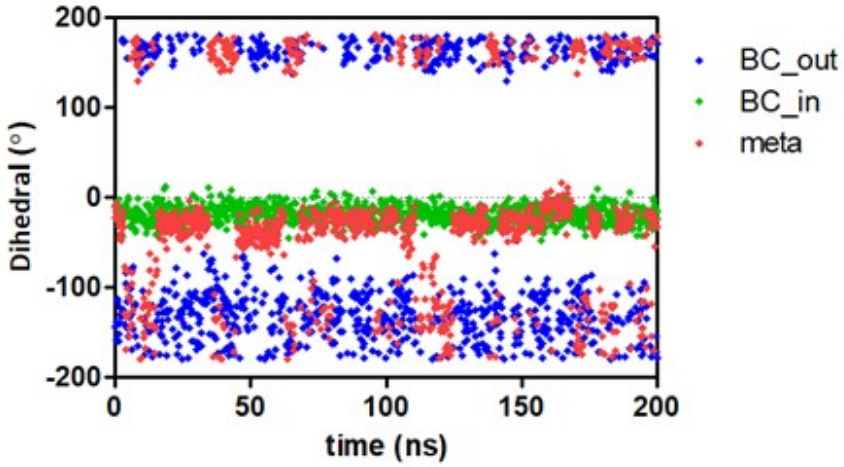

Figure S13. Evolution of the dihedral (N-CA-C-O) Asp1066. Blue: BC-out (unbiased MD simulation, 0-200 ns); Green: BC-in (unbiased MD simulation, 0-200 ns); Red: path metadynamics simulation (600-800 ns).

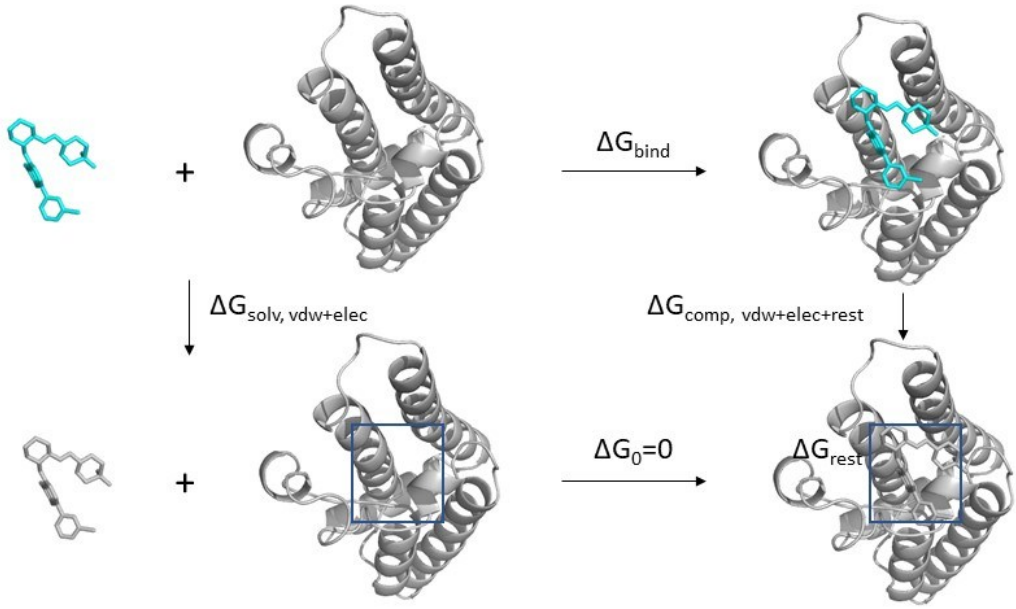

Figure S14. Schematic representation of the thermodynamic cycle for free energy calculations. The interactions (the van der Waals interaction ΔG_{vdw} and electrostatic interaction ΔG_{ele}) of the ligand (cyan) with the solvent as well as with the protein are gradually decoupled with restrain (ΔG_{rest}).

Table S1: ZA dihedral values from the currently available crystal structures of ATAD2's BRD

PDB ID	Ligand	ZA dihedral (°)	Crystallization method
3dai	apo	71.6	Soaking
4qsp	acetyl-lysine	71.2	Soaking
4qsq	DMSO	69.9	Soaking
4qsr	MPD	71.3	Soaking
4qss	N-Methyl-2-pyrrolidone	69.1	Soaking
4qst	1-methylquinolin 2-one	68.6	Soaking
4qsu	Thymine	69.3	Soaking
4qsv	2'-Deoxythymidine	70.5	Soaking
4qsw	5-methyluridine	69.5	Soaking
4qsx	3'-deoxy thymidine	72.1	Soaking
4qut	H4-K(ac)12	75.5	Soaking
4quu	H4-K(ac)5	73.8	Soaking
4tt2	H4(1-20)K5Ac	66.5	Co-crystallization
4tt4	H3(1-21)K14Ac	74.2	Co-crystallization
4tt6	apo	71.5	Co-crystallization
4tte	methyl 3-amino-5-(3,5-dimethyl-1,2-oxazol- 4-yl)benzoate	71.6	Co-crystallization
4tu4	3-(3,5-dimethyl-1,2-oxazol-4-yl)-5-[(phenylsulfonyl)amino]benzoic acid	68.8	Co-crystallization
4tu6	apo	73.6	Co-crystallization
4tyl	5-amino-1,3,6-trimethyl-1,3-dihydro-2H-benzimidazol- 2-one	71.0	Soaking
4tz2	3-(5-phenyl-4H-1,2,4-triazol-3-yl)aniline	73.8	Soaking
4tz8	2-amino-7,7-dimethyl-5,6,7,8-tetrahydro-4H- [1,3]thiazolo[5,4-c]azepin-4-one	71.1	Soaking
5a5n	(2S)-2,6-diacetamido-N-methyl-hexanamide	74.2	Soaking
5a5o	3-METHYL-1,2-DIHYDROQUINOLIN-2-ONE	70.8	Soaking
5a5p	8-{[2-(dimethylamino)ethyl]amino}-3-methyl- 1,2-dihydroquinolin-2-one	70.5	Soaking
5a5q	3-methyl-8-[(piperidin-4-yl)amino]-1,2-dihydro- 1,7-naphthyridin-2-one	70.4	Soaking
5a5r	5-(5-methoxypyridin-3-yl)-3-methyl-8-[(piperidin- 4-yl)amino]-1,2-dihydro-1,7-naphthyridin- 2-one	65.3	Soaking
5a82	8-[[(3R,4R)-3-[[1,1-bis(oxidanylidene)thian- 4-yl]methoxy]piperidin-4-yl]amino]-3-methyl- 1H-1,7-naphthyridin-2-one	68.8	Soaking
5a83	8-[[(3R,4R)-3-[[1,1-bis(oxidanylidene)thian- 4-	66.7	Soaking

	yl]methoxy]piperidin-4-yl]amino]-3-methyl- 5-(5-methylpyridin-3-yl)-1H-quinolin-2-one		
5epb	~{N}-[(2~{S})-2-morpholin-4-ylpropyl]-4-oxidanylidene- 3,5-dihydro-2~{H}-1,5-benzothiazepine-7-carboxamide	65.9	Soaking
5f36	[(2~{R})-1-[(4-ethanoyl-1,3-thiazol-2-yl)amino]- 1-oxidanylidene-propan-2-yl]azanium	68.1	Soaking
5f3a	~{N}-(4-ethanoyl-1,3-thiazol-2-yl)azetidin- 1-ium-3-carboxamide	70.6	Soaking
5lj0	8-(((3R,4R,5S)-3-((4,4-difluorocyclohexyl)methoxy)- 5-methoxypiperidin-4-yl)amino)-3-methyl-5- (5-methylpyridin-3-yl)-1,7-naphthyridin-2(1H)- one	67.3	Soaking

Table S2: Comparison of dihedrals from simulations and the crystal structure data

	MD simulation (º)	PDB structure (º)	PDB ID
Fragment-unbinding	80.0 ± 6.2	70.8	5a5o
Apo	79.6 ± 5.4	71.6	3dai
Fragment-binding	69.2 ± 6.3	70.8	5a5o
Ligand 1-binding	69.8 ± 4.2	66.7	5a83
Peptide-binding	69.9 ± 4.6	66.5	4tt2
Ligand 2-binding	69.8 ± 6.3	68.7	5a81

Table S3: Per-residue contribution obtained from the Glide docking score. All values are in kcal/mol. Vdw represents the van der Waals interaction and ele the electrostatic interaction

	V1013		D1016		E1017		V1018		D1020		Y1021	
	vdw	ele	vdw	ele	vdw	ele	vdw	ele	vdw	ele	vdw	ele
Ligand 1	-3.34	-1.01	-0.18	-0.17	-4.67	-4.33	-3.86	0.02	-0.15	-0.57	-2.03	-0.7
Ligand 2	-2.15	-0.74	-0.04	-0.04	-0.57	-0.71	-2.31	-0.04	-0.15	-0.08	-2.09	-0.7
Peptide	-0.52	-1.21	-0.12	-1.9	-3.66	-3.22	-0.31	-0.03	-0.67	-4.07	-1.33	-2.24

References:

1 Bamborough, P. *et al.* A Chemical Probe for the ATAD2 Bromodomain. *Angew Chem Int Ed Engl* **55**, 11382-11386, doi:10.1002/anie.201603928 (2016).

2 Bamborough, P. *et al.* Structure-Based Optimization of Naphthyridones into Potent ATAD2 Bromodomain Inhibitors. *J Med Chem* **58**, 6151-6178, doi:10.1021/acs.jmedchem.5b00773 (2015).

3 Demont, E. H. *et al.* Fragment-Based Discovery of Low-Micromolar ATAD2 Bromodomain Inhibitors. *J Med Chem* **58**, 5649-5673, doi:10.1021/acs.jmedchem.5b00772 (2015).

4 Fernandez-Montalvan, A. E. *et al.* Isoform-Selective ATAD2 Chemical Probe with Novel Chemical Structure and Unusual Mode of Action. *ACS Chem Biol* **12**, 2730-2736, doi:10.1021/acschembio.7b00708 (2017).